International Journal of Pure and Applied Mathematics

Volume 13 No. 3 2004, 275-291

INHOMOGENEOUS HEAT-CONDUCTION PROBLEMS SOLVED BY A NEW EXPLICIT FINITE DIFFERENCE SCHEME

Matej Praprotnik[1] §, Marjan Šterk[2], Roman Trobec[3]

[1]National Institute of Chemistry
Hajdrihova 19, SI-1001, Ljubljana, SLOVENIA
e-mail: praprot@cmm.ki.si

[2,3]Jožef Stefan Institute
Jamova 39, SI-1000, Ljubljana, SLOVENIA
[2]e-mail: marjan.sterk@ijs.si
[3]e-mail: roman.trobec@ijs.si

Abstract: A heat conduction in systems composed of biomaterials, such as the heart muscle, is described by the familiar heat conduction equation. Due to the inhomogeneity of these materials the equations defining the diffusion problem are difficult to solve. A new explicit finite difference scheme for solving the heat conduction equation for inhomogeneous materials is derived. The new scheme has the same computational complexity as the standard scheme and gives the same solution but with increased resolution of the temperature grid. It was derived and studied on a simple one dimensional problem of heat conduction and applied to studying the temperature distribution in a three dimensional model of the heart muscle.

AMS Subject Classification: 80A20, 65N06
Key Words: heat conduction equation, finite difference scheme, inhomogeneous materials, heart muscle simulation

Received: January 29, 2004

§Correspondence author

1. Introduction

Heat transfer, i.e., energy transport as a result of a temperature gradient, is important in homoeothermic organisms because maintenance of a specific temperature is crucial for their functioning [3]. Because of their complexity, organs, e.g. the heart muscle, are difficult to treat both theoretically and experimentally. Computer simulations based on theoretical physical models [9] are therefore important for understanding heat transfer processes in such systems. There are three fundamental heat transfer mechanisms: conduction, convection, and radiation. Conduction, described by the heat conduction equation, is usually the most important for thermal energy transport within a solid substance. In order to study the temperature distribution in a system, such as the heart muscle, efficient numerical schemes for solving the heat conduction equation are required [6]. The heat conduction equation describes conduction on the macroscopic scale and the numerical schemes are usually based on the finite difference approximation [12] as opposed, for example, to molecular dynamics simulations [1], where the properties of the physical system are computed on the microscopic scale, and efficient algorithms for solving the Hamilton equations for each atom in the system are used [7].

The structure of this paper is as follows. In the next section, the standard schemes are described and a new explicit finite difference scheme for solving the heat conduction equation for arbitrary inhomogeneous materials is derived. The results of simulating heat diffusion in one dimensional (1-D) heat conductors composed of different materials and in a realistic three-dimensional (3-D) heart model are presented in Section 3. The paper concludes with a discussion of the results and directions for future work.

2. Methods

The basic equation that describes heat transfer is known as the heat conduction equation [11]

$$\nabla \cdot (\boldsymbol{\lambda} \nabla T) = \rho c_p (\frac{\partial T}{\partial t} + (\mathbf{v} \cdot \nabla) T), \tag{1}$$

where $\nabla = (\frac{\partial}{\partial x}, \frac{\partial}{\partial y}, \frac{\partial}{\partial z})$ is a differential operator in terms of Cartesian coordinates, $\mathbf{v}$ is the velocity of a part of the substance volume, $\rho = \rho(\mathbf{r})$ is the mass density, and $c_p = c_p(\mathbf{r})$ is the specific heat at constant pressure. $\boldsymbol{\lambda} = \boldsymbol{\lambda}(\mathbf{r}, T)$ is the heat conductivity of a substance, which is usually temperature dependent. Although (1) is in general nonlinear, we focus here only on the linear cases

where $\boldsymbol{\lambda} = \boldsymbol{\lambda}(\mathbf{r})$. $\boldsymbol{\lambda}$ is in general a 3×3 tensor. For isotropic substances $\boldsymbol{\lambda} = \lambda \boldsymbol{I}$ and $\nabla \boldsymbol{\lambda} = \nabla \lambda$ hold, and in this case λ can be treated as a scalar. $\boldsymbol{I}$ denotes the 3×3 identity matrix. $T = T(\mathbf{r}, t)$ is the temperature as a function of the position $\boldsymbol{r} = (x, y, z)$ and time t.

For a 1-D system which is motionless (1) is written as

$$\rho c_p \frac{\partial T}{\partial t} = \lambda(x) \frac{\partial^2 T}{\partial x^2} + \frac{\partial \lambda(x)}{\partial x} \cdot \frac{\partial T}{\partial x}, \tag{2}$$

or equivalently

$$\rho c_p \frac{\partial T}{\partial t} = \frac{\partial}{\partial x} \left[\lambda(x) \frac{\partial T}{\partial x} \right]. \tag{3}$$

(2) can be used for determining the stationary temperature distribution in a 1-D heat conductor of length l shown in Figure 1. The conductor is composed

Figure 1: A 1-D heat conductor composed of two materials with the same thickness but different λ, ρ, and c_p

of two different materials of the same thickness. The boundary conditions at the left and right end are the temperatures T_L and T_R, respectively. The left part of the conductor is composed of a substance with λ_1, ρ_1, and c_{p_1}, and the substance of the right part is characterized by λ_2, ρ_2, and c_{p_2}. This simple system provides an excellent test case for analysis of different methods because they can be compared to the analytical solution. Also, the difference between correct and incorrect solutions is diminished in more complex systems, as is shown by the numerical results of a heat conduction simulation in heart muscle in Section 3.

2.1. Analytical Solution

The analytical solution, which is used as the reference to check the accuracy of the numerical solution, can be derived as follows. In the stationary state

$$0 = \frac{\partial T}{\partial t} = D \frac{\partial^2 T}{\partial x^2} \tag{4}$$

holds for each separate part of the conductor. D is the thermal diffusivity of the substance defined as $D = \lambda/(\rho c_p)$. The boundary conditions are $T(0) = T_L$,

$T(l) = T_R$ and the transient conditions between the left and right part of the conductor are

$$T_1(l/2) = T_2(l/2), \tag{5}$$

$$\lambda_1 \frac{\partial T_1}{\partial x}|_{l/2} = \lambda_2 \frac{\partial T_2}{\partial x}|_{l/2}, \tag{6}$$

which state that the temperature at the point of contact is the same for both parts and that the heat flux density, determined by the Fourier Law of heat transfer [4], is conserved. The solution of (4) comprises the linear functions

$$T_1 = A_1 x + T_L, \tag{7}$$

$$T_2 = A_2(x - l) + T_R. \tag{8}$$

Inserting (7) and (8) into (5) and (6) the constants A_1 and A_2 are

$$A_1 = \frac{2(T_R - T_L)}{l(\frac{\lambda_1}{\lambda_2} + 1)}, \tag{9}$$

$$A_2 = \frac{2(T_R - T_L)}{l(\frac{\lambda_2}{\lambda_1} + 1)}, \tag{10}$$

and

$$T_2(l/2) = \frac{\lambda_1 T_L + \lambda_2 T_R}{\lambda_1 + \lambda_2}. \tag{11}$$

The temperature profile has the shape of a linear function that is broken at the contact point between the two different parts of the conductor.

2.2. Finite Difference Scheme with Gradient Term

For the numerical solution of (2) the following explicit finite difference scheme can be used

$$\rho_i c_{p_i} \frac{T_i^{n+1} - T_i^n}{\Delta t} = \lambda_i \frac{T_{i+1}^n - 2T_i^n + T_{i-1}^n}{\Delta x^2} + \frac{(\lambda_{i+1} - \lambda_{i-1})(T_{i+1}^n - T_{i-1}^n)}{4\Delta x^2}. \tag{12}$$

Index i denotes the spatial discretization and Δx is the step size. Index n refers to the time discretization and Δt is the length of the time step. If there were no gradient term in (12), i.e. the last term on the right side of (12), this scheme would be stable for time steps up to $\Delta t = \Delta x^2/(2D_{max})$, where

D_{max} is the maximal value of thermal diffusivity in the system. The gradient term $\frac{\partial\lambda}{\partial x}\cdot\frac{\partial T}{\partial x}$ introduces instability into the system if the difference between the thermal conductivities of two sequential grid points is not small enough. The gradient term $\frac{(\lambda_{i+1}-\lambda_{i-1})(T^n_{i+1}-T^n_{i-1})}{4\Delta x^2}$ can take very large values in these cases and the approach in (12) is expected to become unstable [8].

2.3. Standard Finite Difference Scheme

The explicit finite difference scheme [10, 5] for a nonlinear diffusion equation

$$\rho c_p\frac{\partial T}{\partial t}=\frac{\partial}{\partial x}\left[\lambda(T)\frac{\partial T}{\partial x}\right], \tag{13}$$

based on the finite-difference approximation for derivatives [12] is

$$\begin{aligned}\rho_i c_{p_i}\frac{T^{n+1}_i-T^n_i}{\Delta t}&=\frac{\lambda_{i-1/2}\frac{T^n_{i-1}-T^n_i}{\Delta x}+\lambda_{i+1/2}\frac{T^n_{i+1}-T^n_i}{\Delta x}}{\Delta x}\\&=\frac{\lambda_{i-1/2}(T^n_{i-1}-T^n_i)+\lambda_{i+1/2}(T^n_{i+1}-T^n_i)}{\Delta x^2},\end{aligned} \tag{14}$$

where

$$\lambda_{i\pm1/2}=\frac{\lambda_i+\lambda_{i\pm1}}{2}. \tag{15}$$

Because in (3) $\lambda=\lambda(x)$, as opposed to $\lambda=\lambda(T)$ in (13), (15) cannot be used for calculating $\lambda_{i\pm1/2}$ when solving (3).

We therefore consider the heat flux P through the conductor of length l and cross sectional area S [4] as

$$P=-\frac{\lambda S}{l}\Delta T, \tag{16}$$

where ΔT is the temperature difference between the ends of the conductor. The heat resistance is defined as

$$R=\frac{l}{\lambda S}. \tag{17}$$

The relation between the heat flux and the temperature difference is analogous to Ohm Law in the case of an electrical current through a resistor R

$$P=-\frac{\Delta T}{R}, \tag{18}$$

where the temperature difference corresponds to the voltage. From this analogy the equations for the different configurations of heat resistors can be derived – the total resistance of serial resistors is the sum of individual resistances, while in the case of parallel resistors the total resistance is the sum of their reciprocal values. The total heat conductivity λ_c of two serial heat resistors with the heat conductivities λ_1 and λ_2 is therefore

$$\frac{2}{\lambda_c} = \frac{1}{\lambda_1} + \frac{1}{\lambda_2}. \tag{19}$$

For solving (2) or (3) we use the standard explicit finite difference scheme (14), where $\lambda_{i\pm1/2}$ are determined as in (19)

$$\frac{2}{\lambda_{i\pm1/2}} = \frac{1}{\lambda_i} + \frac{1}{\lambda_{i\pm1}}. \tag{20}$$

Note that $\lambda_{i+1/2}$ is equal to $\lambda_{i-1/2}$ of the next grid element and need not be calculated separately.

2.4. New Explicit Finite Difference Scheme

In developing the new explicit finite difference scheme a similar approach to that in deriving the analytical solution is used. The heat conduction equation without the trouble some gradient term $\frac{\partial\lambda}{\partial x} \cdot \frac{\partial T}{\partial x}$ is solved for each grid element of the conductor separately because they are homogeneous. The separate solutions are then smoothly matched by transient conditions at the contact. The transient condition for the equality of the temperatures at the contact point is fulfilled by introducing a new intermediate grid point $T_{i+1/2}$ that lies on the boundary between grid elements as shown in Figure 2. The temperature at the boundary $T_{i+1/2}$ is derived from the transient condition for the heat flux density using (6)

$$\lambda_i \frac{\partial T_i}{\partial x}|_\Omega = \lambda_{i+1} \frac{\partial T_{i+1}}{\partial x}|_\Omega, \tag{21}$$

$$\lambda_i \frac{T_{i+1/2} - T_i}{\frac{\Delta x}{2}} = \lambda_{i+1} \frac{T_{i+1} - T_{i+1/2}}{\frac{\Delta x}{2}}, \tag{22}$$

$$T_{i+1/2} = \frac{\lambda_i T_i + \lambda_{i+1} T_{i+1}}{\lambda_i + \lambda_{i+1}}, \tag{23}$$

where Ω denotes the boundary and index i the grid point, where the jump in thermal conductivity occurs. The second derivative of the temperature at the

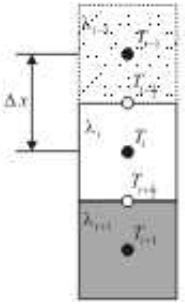

Figure 2: Grid elements with different λ, ρ, and c_p, denoted by different patterns in the grid elements

grid points far from the boundary is computed as

$$\frac{\partial^2 T_i}{\partial x^2} = \frac{T_{i+1} - 2T_i + T_{i-1}}{\Delta x^2}, \tag{24}$$

while at the grid point near the boundary it is defined as

$$\frac{\partial^2 T_i}{\partial x^2} = \frac{\frac{T_{i+1/2} - T_i}{\frac{\Delta x}{2}} - \frac{T_i - T_{i-1/2}}{\frac{\Delta x}{2}}}{\Delta x} = \frac{2(T_{i+1/2} - 2T_i + T_{i-1/2})}{\Delta x^2}. \tag{25}$$

In (25) the left and right differences were used for the first derivatives in the grid points $T_{i+1/2}$ and $T_{i-1/2}$, respectively. Thus only the temperatures from the same grid element are used in order to avoid the troublesome gradient term $\frac{\partial \lambda}{\partial x} \cdot \frac{\partial T}{\partial x}$. If $\lambda_i = \lambda_{i-1} = \lambda_{i+1}$ then (25) simplifies to (24). $T_{i-1/2}$ is, analogously to (23), defined as

$$T_{i-1/2} = \frac{\lambda_i T_i + \lambda_{i-1} T_{i-1}}{\lambda_i + \lambda_{i-1}}. \tag{26}$$

An iterative solution procedure is as follows: first, $T_{i+1/2}$ and $T_{i-1/2}$ are computed from the temperatures from the previous step by (23) and (26). Note that $T_{i+1/2}$ is equal to $T_{i-1/2}$ of the next grid element and need not be calculated separately. Then (25) is used to compute the second derivatives in the heat conduction equation (2). In this manner the separate solutions for each grid element, which itself is homogeneous, are smoothly matched together. The troublesome gradient term $\frac{\partial \lambda}{\partial x} \cdot \frac{\partial T}{\partial x}$ is thus omitted in the heat conduction equation, (2). One does not have to consider how and to what extent the heat conductivity varies with position. The transient conditions are also considered implicitly. Some unnecessary extra computation is performed for calculating $T_{i+1/2}$ and $T_{i-1/2}$ in parts where the substance is homogeneous. It is interesting

that (25) for an inhomogeneous substance is similar to (24) for a homogeneous substance. The only difference is the use of weighted temperature averages in (25), as expressed in (26) and (23).

The new explicit finite difference scheme is defined as

$$\rho_i c_{p_i} \frac{T_i^{n+1} - T_i^n}{\Delta t} = \lambda_i \frac{2(T_{i+1/2}^n - 2T_i^n + T_{i-1/2}^n)}{\Delta x^2}, \tag{27}$$

where $T_{i+1/2}$ and $T_{i-1/2}$ are computed according to (23) and (26), respectively. Note that the new scheme, (27), gives the same solution as the standard scheme, (14), only here $T_{i+1/2}$ and $T_{i-1/2}$ are computed instead of $\lambda_{i+1/2}$ and $\lambda_{i-1/2}$. This has the advantage of increasing the resolution of the temperature grid, which is the solution of the problem, as opposed to the standard scheme, where the extra calculation provides no additional information. The computational complexity of the new scheme remains the same as in the standard scheme.

For the 3-D example (2) is generalized to

$$\rho c_p \frac{\partial T}{\partial t} = \lambda \left(\frac{\partial^2 T}{\partial x^2} + \frac{\partial^2 T}{\partial y^2} + \frac{\partial^2 T}{\partial z^2} \right) + \frac{\partial \lambda}{\partial x} \cdot \frac{\partial T}{\partial x} + \frac{\partial \lambda}{\partial y} \cdot \frac{\partial T}{\partial y} + \frac{\partial \lambda}{\partial z} \cdot \frac{\partial T}{\partial z}, \tag{28}$$

where $\lambda = \lambda(x, y, z)$ and $T = T(x, y, z)$. (28) is a 3-D analogue of (2) in the case of 1-D. (28) can be rearranged to

$$\rho c_p \frac{\partial T}{\partial t} = \left(\lambda \frac{\partial^2 T}{\partial x^2} + \frac{\partial \lambda}{\partial x} \cdot \frac{\partial T}{\partial x} \right) + \left(\lambda \frac{\partial^2 T}{\partial y^2} + \frac{\partial \lambda}{\partial y} \cdot \frac{\partial T}{\partial y} \right) + \left(\lambda \frac{\partial^2 T}{\partial z^2} + \frac{\partial \lambda}{\partial z} \cdot \frac{\partial T}{\partial z} \right). \tag{29}$$

By comparing (29) with (2) and by virtue of (27), the new explicit finite difference scheme for a inhomogeneous 3-D example yields the form

$$\rho_{i,j,k} c_{p_{i,j,k}} \frac{T_{i,j,k}^{n+1} - T_{i,j,k}^n}{\Delta t} = 2\lambda_{i,j,k} \left(\frac{T_{i+1/2,j,k}^n - 2T_{i,j,k}^n + T_{i-1/2,j,k}^n}{\Delta x^2} + \frac{T_{i,j+1/2,k}^n - 2T_{i,j,k}^n + T_{i,j-1/2,k}^n}{\Delta y^2} + \frac{T_{i,j,k+1/2}^n - 2T_{i,j,k}^n + T_{i,j,k-1/2}^n}{\Delta z^2} \right). \tag{30}$$

Indices i, j, k denote the spatial discretization in the x, y, and z directions, respectively, $\Delta x, \Delta y, \Delta z$ are the corresponding step sizes, and

$$T_{i\pm1/2,j,k} = \frac{\lambda_{i,j,k}T_{i,j,k} + \lambda_{i\pm1,j,k}T_{i\pm1,j,k}}{\lambda_{i,j,k} + \lambda_{i\pm1,j,k}}. \tag{31}$$

$T_{i,j\pm1/2,k}$ and $T_{i,j,k\pm1/2}$ are defined similarly.

3. Results

All four approaches for solving the heat conduction equation described in the previous section were tested on the 1-D heat conductor presented in Figure 1. The temperature profile was also computed for the case of neglecting $\frac{\partial\lambda}{\partial x} \cdot \frac{\partial T}{\partial x}$ in (2) in order to check the importance of this term.

The new explicit scheme, generalized to 3-D, was also applied to computing the temperature distribution in heart muscle. It was compared to the standard scheme and to previous results [13], where the gradient term was neglected.

3.1. 1-D Heat Conductor

In order to better understand the heat conduction in a complex system of heart muscle the substance constants λ_1, ρ_1, and c_{p_1} were chosen to correspond to water and λ_2, ρ_2, and c_{p_2} to pericardium (see Table 1).

	$\lambda \left[\frac{W}{Km}\right]$	$\rho \left[\frac{kg}{m^3}\right]$	$c_p \left[\frac{J}{kgK}\right]$
Water	0.555	1000	4219
Blood	0.490	1010	3826
Blood vessels	0.360	1100	3826
Muscle tissue	0.590	1100	3966
Pericardium	0.360	1100	2761
Fat	0.200	1100	2275
Air	0.025	1.29	716

Table 1: λ, ρ, and c_p of substances in human heart [13] (pericardium is the thin membrane that surrounds the heart)

All the constants and the temperatures $T_L = 273.2K$, $T_R = 285K$ were taken from the experimental values for heart muscle [13]. The length of the time step was set to $\Delta t = \Delta x^2/(6D_{max})$, and the computation was stopped

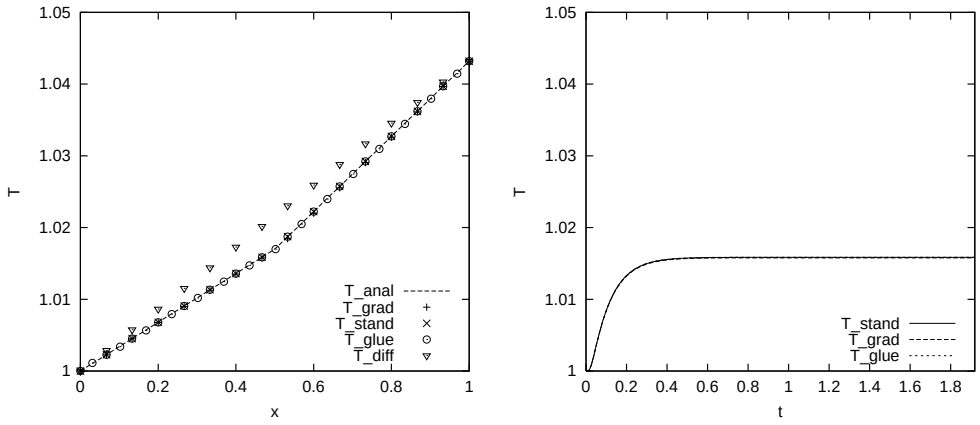

(a) (b)

Figure 3: Results for a 1-D heat conductor composed of water and pericardium. Figure (a) shows the temperature profile. The temperature is dimensionless and is measured in units of the temperature of water at the left boundary of the conductor. On the x axis the normalized length of the conductor is presented. Figure (b) shows relaxation of the temperature in the grid element next to the contact between water and pericardium until the convergence condition is fulfilled. The time is measured in $t_0 = l^2/D_{water}$ units. The length of the time step is $1.6667 \cdot 10^{-5}\, t_0$.

when the convergence condition $T_{n-1}^{n+1} - T_{n-1}^{n} < \epsilon = 10^{-15}$ was fulfilled. The resulting temperature profile is presented in Figure 3(a). T_{anal} is the analytical solution, T_{grad} is the numerical solution using (12), T_{stand} is the numerical solution using the standard finite difference scheme, (14), T_{glue} is the numerical solution obtained by the new finite difference scheme, (27), and T_{diff} is the numerical solution obtained by neglecting the gradient term in (2). It can be seen from Figure 3(a) that the gradient term plays an important role, since the solution T_{diff} corresponds to the solution of a homogeneous conductor regardless of the thermal conductivity of the conductor. If the gradient term is considered as in (12) then the solution agrees with the analytical solution. Because water and pericardium have similar thermal conductivities no stability problems occur. Figure 3(a) shows that solutions obtained by the standard and new explicit finite difference schemes also agree with the analytical solution. Figure

3(b) displays the time relaxation to the stationary value of the temperature at the grid element next to the contact between water and pericardium. It can be seen that solutions obtained by different numerical schemes converge equally fast to the stationary temperature.

The temperature profile and relaxation were also computed for the example of a 1-D heat conductor composed of water and air (see Table 1) with boundary conditions $T_L = 273.2K$, $T_R = 295K$, where the difference between thermal conductivities is much larger than in the case of water and pericardium. The numerical solution obtained by (12) is not stable in this case due to the large value of $\frac{\partial \lambda}{\partial x} \cdot \frac{\partial T}{\partial x}$ at the contact between water and air. On the contrary Figure 4(a) shows that the numerical solutions obtained by the standard and the new finite difference scheme accurately determine the temperature profile. In Figure

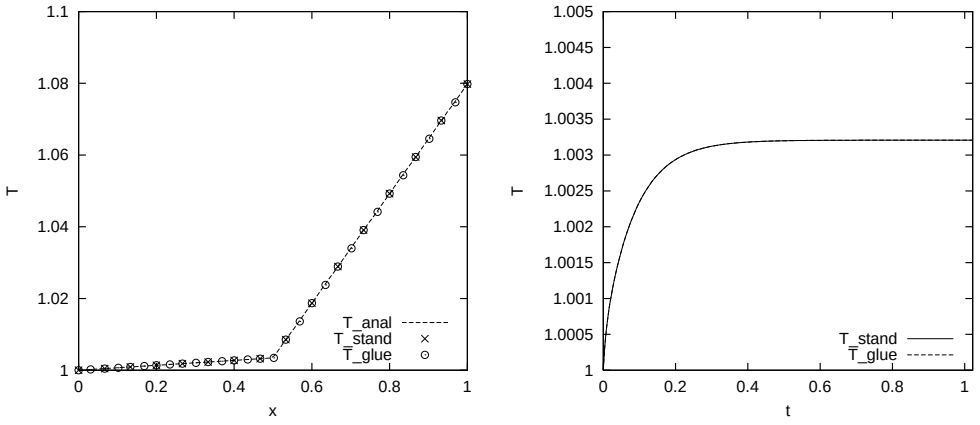

(a) (b)

Figure 4: The temperature profile for a 1-D heat conductor composed of water and air (a) and relaxation of the temperature in the grid element next to the contact between water and air (b). The axes and units are the same as in Figure 3. The length of the time step is $8.1079 \cdot 10^{-8}\, t_0$.

4(b) the time relaxation of the temperature to the stationary value in the grid element next to the contact between water and air value is presented. Note that the standard and the new schemes converge equally fast.

In Figure 5(a) the example of a heat conductor composed of water and pericardium and one grid point of air in between them is presented. The boundary conditions were chosen as $T_L = 273.2K$, $T_R = 285K$. As can be seen from Fig-

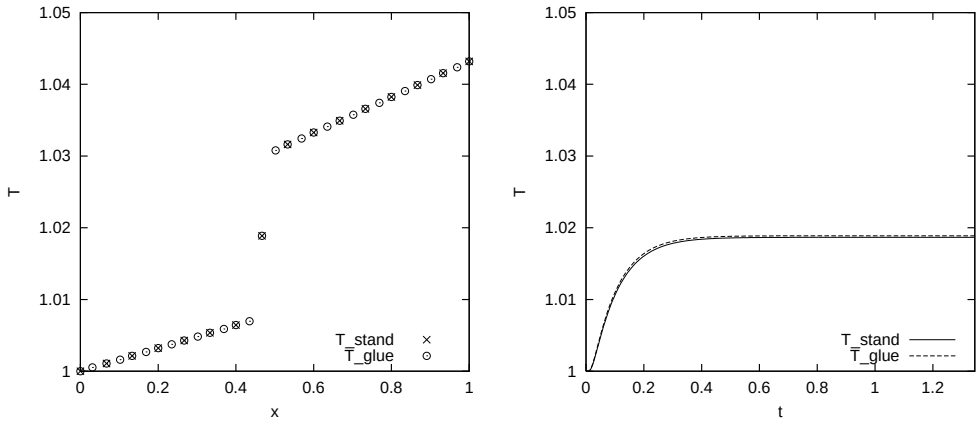

(a) (b)

Figure 5: The temperature profile for a 1-D heat conductor composed of water and pericardium with an isolation grid point of air (a) and relaxation of the temperature in the air grid point (b). The axes and units are the same as in Figure 3. The length of the time step is $8.1079 \cdot 10^{-8}\, t_0$.

ure 5(a) the standard and the new scheme give the same temperature profile for this example also. The insulative nature of air can also be observed. Figure 5(b) shows the time relaxation of the temperature at the air grid point. From Figures 3,4 and 5 it can be concluded that the total relaxation time in the case when air is present in the system is shorter. The total number of iterations, however, is higher due to the shorter time step used.

3.2. Heart Muscle

The new scheme for the 3-D example (30) was also tested on a heart cooling simulation. During a non-beating heart operation, local hypothermia is used to slow down the tissue metabolism and thus allow for a longer operation without damaging the tissue [2]. In order to provide adequate protection to all heart tissues, they have to be uniformly cooled down and no part of the heart tissue should stay warm. Uniform temperature distribution is also important because areas with different temperatures are often origins of cardiac arrhythmias. One of the ways to cool the tissues is local topical cooling, which is applied with cold saline solution, with or without ice slush, around the heart.

A three-dimensional computer heart model, derived from Visible Human Dataset, National Library of Medicine was used. The model is made from cubes with spatial resolution of 1 mm. Figure 6 shows a heart cross-section and the initial conditions used, which were the same as those taken in [13]. The temperature profile resulting from simulations with the new scheme can be seen in Figure 7(b). We compared it to the results from [13], where the gradient term in (28) was neglected (see Figure 7(a)) but which cannot be dismissed as incorrect without seeing the correct results. Only after careful comparison can one find out that neglecting the gradient term in (2) overestimates heat transfer from the heart to the cooling media by a significant amount. The same effect as in a 1-D heat conductor (Figure 3) is also noticeable, i.e. the results are the same as if all the materials had the same thermal diffusivity, thus object shapes are not reflected in the temperature profile. The difference is more readily seen in Figure 8, where dark and light shading represent the areas, where the scheme with the neglected gradient term gives lower and higher temperatures, respectively.

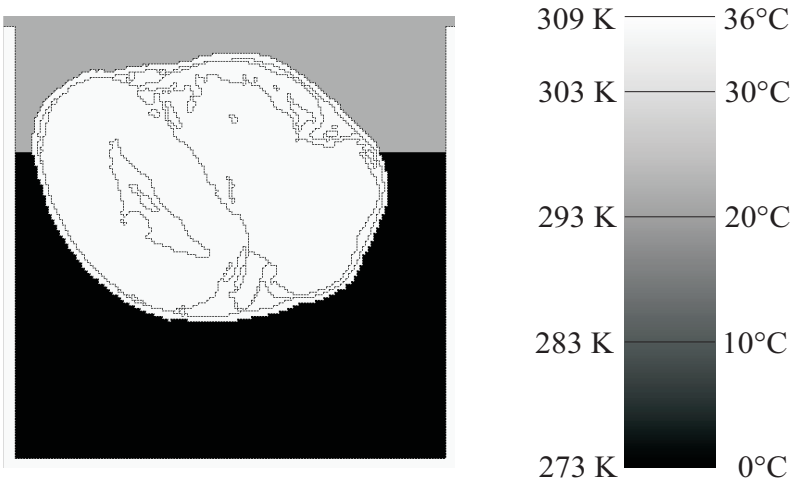

Figure 6: Initial temperature profile of the heart (308 K) before cooling. The cooling media are water (constant temperature 273 K) below the heart and air (initial temperature 295 K) above it. The model is surrounded by a box with constant temperature 308 K.

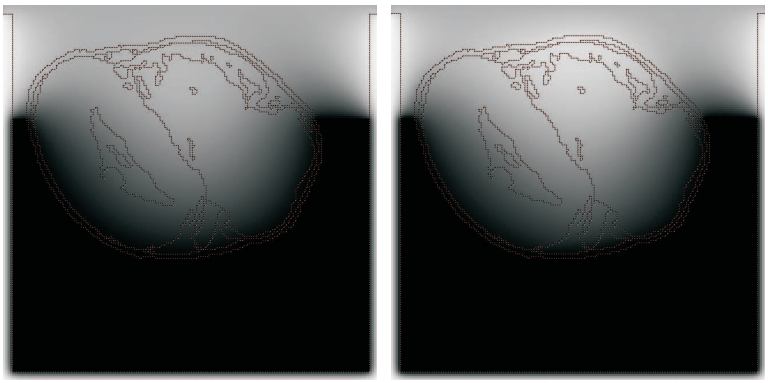

(a) (b)

Figure 7: Temperature profile of the heart after 1 hour neglecting the gradient term (a) and using the new scheme (b). The temperature scale is the same as in Figure 6.

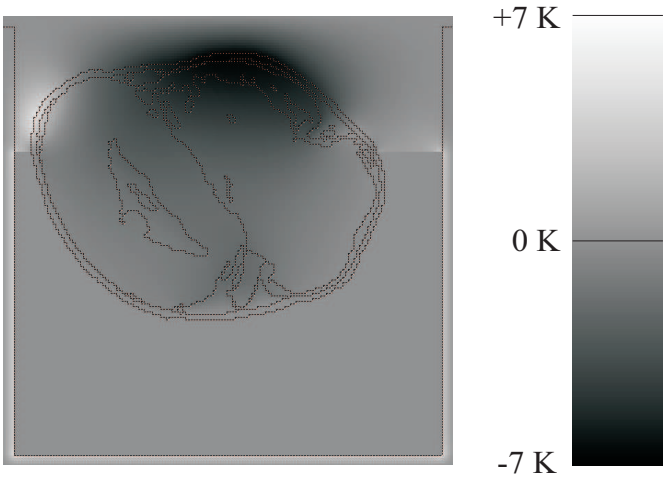

Figure 8: The error resulting from neglecting the gradient term in a 1-hour heart cooling simulation.

4. Conclusions

In this paper a new explicit finite difference scheme for inhomogeneous diffusion problems is developed and compared to standard schemes. The new approach is similar to the analytical solution in that two solutions for homogeneous parts are smoothly matched together by a transient condition. In this approach, each separate grid point is considered as the homogeneous part, and the transient condition is used to obtain the solution. The method was illustrated on an example of a 1-D heat conductor composed of different substances found in heart muscle and its environment. It was also generalized to 3-D and applied to computating the temperature profile in a heart muscle. The simulation results show that the new scheme not only accurately determines the temperature profile, but gives the same solution as the standard scheme with improved resolution. The computational complexity of the two schemes is the same. In the standard scheme the additional computation of weighted average of heat conductivities has to be performed, which provides no additional information. In the new scheme, however, the weighted average of temperatures is computed, which doubles the resolution of the temperature grid.

Acknowledgement

The authors express their thanks to Dr. Dušanka Janežič for stimulating discussions. This research was funded under Grant No. P2-0095 and P1-0002 by the Ministry of Education, Science and Sports of Slovenia.

References

[1] M.P. Allen, D.J. Tildesley, *Computer Simulation of Liquids*, Clarendon Press, Oxford (1987).

[2] I. Birdi, M. Caputo, G. Underwood, D. Angelini, A. Bryan, Influence of normothermic systemic perfusion temperature on cold myocardial protection during coronary artery bypass surgery, *Cardiovascular Surgery*, **7** (1999), 369-374.

[3] H.F. Bowman, E.G. Cravalho, M. Woods, Theory, measurement, and application of thermal properties of biomaterials, *Ann. Rev. Biophysics-Bioengineering*, **4** (1975), 43-80.

[4] H.S. Carslaw, J.C. Jaeger, *Conduction of Heat in Solids*, Oxford University Press, London (1959).

[5] C.F. Gonzalez-Fernandez, F. Alhama, M. Alarcon, J.F. Lopez-Sanches, Digital simulation of transient heat conduction with polynomial variable thermal conductivity and specific heat, *Computer Physics Communications*, **111** (1998), 53-58.

[6] M.T. Heath, *Scientific Computing: An Introductory Survey*, Second Edition, WCB/McGraw-Hill (2002).

[7] D. Janežič, M. Praprotnik, Symplectic molecular dynamics integration using normal mode analysis, *Int. J. Quant. Chem.*, **84** (2001), 2-12.

[8] I. Kuščer, A. Kodre, *Mathematik in Physik und Technik*, Springer-Verlag, Berlin (1993).

[9] J.W. Mitchell, G.E. Myers, An analytical model of the counter-current heat exchange phenomena, *Biophysical Journal*, **8** (1968), 897-911.

[10] M.N. Özisik, *Finite Difference Methods in Heat Transfer*, CRC Press, Boca Raton (1994).

[11] G.B. Pollard, *Lectures on Partial Differential Equations*, Wiley, New York (1964).

[12] W.H. Press, B.P. Flannery, S.A. Teukolsky, W.T. Vetterling, *Numerical Recipes. The Art of Scientific Computing*, Cambridge University Press, Cambridge (1986).

[13] R. Trobec, B. Slivnik, B. Geršak, T. Gabrijelčič, Computer simulation and spatial modelling in heart surgery, *Computers in Biology and Medicine*, **4** (1998), 393-403.